

A Compact UWB Printed Monopole MIMO Antenna with Mutual Coupling Reduction

Hossein Babashah¹, Hamid R. Hassani¹, and Sajad Mohammad-Ali-Nezhad^{2, *}

Abstract—A compact multiple-input-multiple-output (MIMO) antenna with very high isolation is proposed for ultrawideband (UWB) applications. The antenna with a compact size of $30.1 \times 20.5 \text{ mm}^2$ ($0.31\lambda_0 \times 0.21\lambda_0$) consists of two planar-monopole antenna elements. It is found that isolation of more than 25 dB can be achieved between two parallel monopole antenna elements. For the low-frequency isolation, an efficient technique of bending the feed-line and applying a new protruded ground is introduced. To increase isolation, a design based on suppressing surface wave, near-field, and far-field coupling is applied. The simulation and measurement results of the proposed antenna with the good agreement are presented and show a bandwidth with $S_{11} \leq -10 \text{ dB}$, $S_{12} \leq -25 \text{ dB}$ ranged from 3.1 to 10.6 GHz making the proposed antenna a good candidate for UWB MIMO systems.

1. INTRODUCTION

MIMO technology has aroused interest because of its application in 4G, RFID, Digital Home, and WLAN. Demand for high data rate and, as a result, huge bandwidth is increasing. In 2002 US-FCC approved unlicensed use of 3.1–10.6 GHz frequency band at low energy level [1]. Therefore in order to improve the capacity of the system, UWB MIMO antenna has been developed for commercial systems. UWB MIMO antenna with high isolation has application in short-range high-data-rate, transmission automotive communications, and radar imaging systems [2, 3].

When several antennas are in close proximity, they suffer from severe mutual coupling, which results in lower antenna efficiency and loss of bandwidth, and further degrades the performance of either diversity gain or spatial multiplexing schemes [3]. So the question then arises as to how to put together antenna elements with low coupling and occupying the least possible space. Because these two properties contradict each other, the problem is very challenging. The mutual coupling is also attributed to three phenomena: near-field coupling, far-field coupling, and surface wave coupling [4].

Many techniques and MIMO structures have been proposed for compact MIMO systems. In [5–7], the size of the proposed antenna was not small enough for the present portable devices. In [8, 9], the proposed antenna was not able to cover the entire UWB bandwidth allocated by the FCC [1]. In [3, 5] and [10–13] unlike our purposed antenna, the antenna elements were perpendicular to each other. None of the above could attain a very high isolation with $S_{12} < -30 \text{ dB}$ in such a small size while covering the whole UWB bandwidth.

Certain techniques are also reported to improve isolation. Methods include using simple and fractal-based DGS [14], EBG [15], soft surface structures [16], and Metamaterial-Inspired Isolatorin between the antenna elements [17], etc.

Among the aforementioned designs, none of them could achieve very high isolation in such a small size at low-frequency levels because in small size structures reducing mutual coupling at these frequencies due to long wavelength is very challenging.

Received 9 January 2019, Accepted 14 February 2019, Scheduled 12 March 2019

* Corresponding author: Sajad Mohammad-Ali-Nezhad (s.mohammadalinezhad@qom.ac.ir).

¹ Electrical and Electronics Engineering Department, Shahed University, Tehran, Iran. ² Electrical and Electronics Engineering Department, University of Qom, Qom, Iran.

feed line. Two H-shaped symmetric slots are protruded in the ground to engineer field pattern causing mutual coupling. This reduction happens because of the electromagnetic wave experiences discontinuity along its way of propagation which also results in radiation [18]. Two symmetric short strips are also etched in the ground to improve impedance matching. To attain high isolation at the higher frequencies, the grounds are separated by protruding the common ground with dimensions of $L_g \times L_{g3}$, and this will attenuate near-field coupling.

In order to fabricate the antenna, the dimensions are optimized for both isolation and compact size. The fabricated proposed antenna is shown in Figure 2. Table 1 shows the dimension of the proposed antenna.

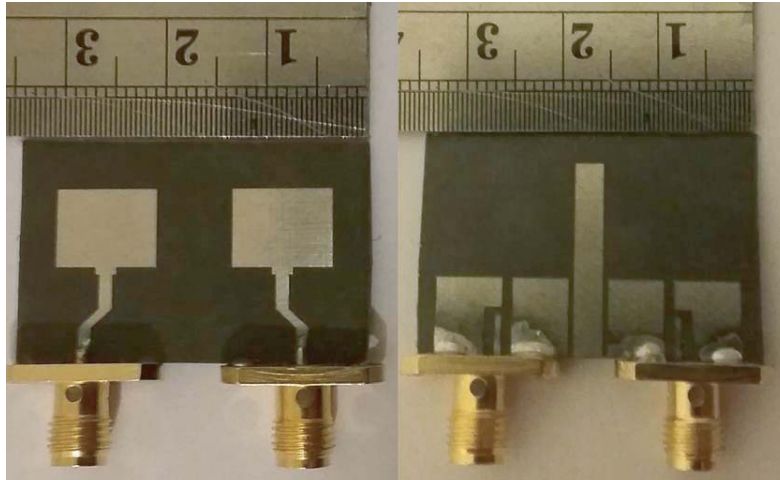


Figure 2. Photograph of top and bottom view of the fabricated antenna.

Table 1. Dimensions of the proposed antenna in (mm).

W_r	L_r	W_m	L_m	L_f	L_{s1}	L_{s2}	L_g	D_f
10	8	2.1	0.7	9.35	4	4.6	7.4	4.1
L	W	W_s	W_{s1}	W_a	L_{f1}	L_s	L_{g3}	L_{g1}
20.5	30.1	3	0.7	19.2	3.5	19	0.5	1

3. MUTUAL COUPLING REDUCTION WORKING MECHANISM

Mutual coupling deteriorates the performance of UWB MIMO antenna [19]. To overcome this limitation, the origination of mutual couplings in UWB MIMO antennas is described, and they are summarized in three phenomena including far-field coupling, near field coupling, and surface wave coupling [4]. To enhance the isolation between the monopole antenna elements, this paper goes through each of the causes of mutual coupling and gives a solution to prevent the effect. To this end, first, surface wave coupling is omitted by just adjusting the dielectric thickness, and then far-field coupling is inhibited using radiation pattern engineering through slots and slits after the near-field contribution to coupling is relaxed by making the monopole antenna element far enough to avoid coupling due to the near-field phenomenon. The in-depth explanations of these methods are described as follows.

To prevent surface wave coupling, the physics behind exciting propagation mode within the dielectric is taken, meaning that surface waves are excited in the patch antenna, and they consist of several modes [18]. The number of modes is attributed to the dimension of the dielectric slab, and the smaller the slab thickness is, the fewer the excited surface modes are in the waveguide. For instance, a surface wave cannot exist when there is no dielectric slab to support them. Moreover, higher order

modes of surface waves are excited as the substrate thickness or permittivity increases. Therefore, an approach to increase isolation due to surface wave is reducing the dielectric thickness or permittivity. Here, a thin thickness of 0.787 mm is selected, and a Rogers substrate with relative permittivity of 2.2 is used.

Through the following, one can analyze the level of surface wave propagation. If the dielectric between the antenna elements is removed, the air between the patch elements eliminates the surface wave propagation. Accordingly, any difference between S_{12} values of the antenna structure with and without the dielectric implies surface wave effects, for an illustration of this surprising behavior (see Figure 3). Nevertheless, as shown in Figure 3, mutual coupling still exists between the antenna elements. Accordingly, this coupling may contribute to near-field and far-field couplings.

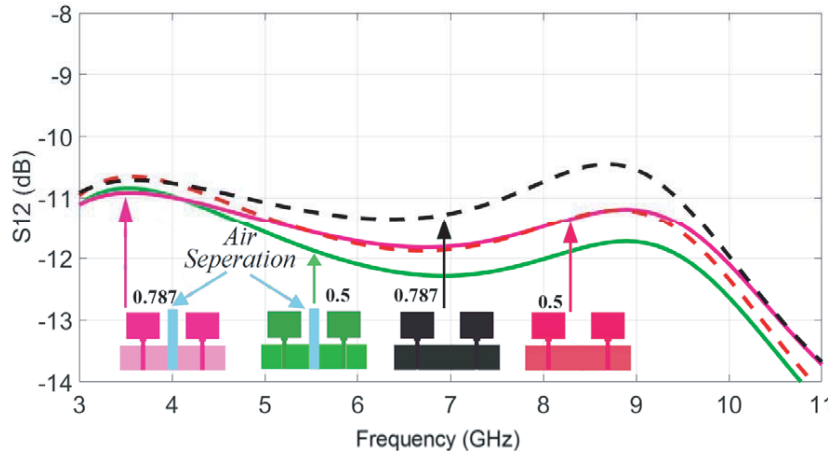


Figure 3. Effect of thickness and air separation on surface wave causing mutual coupling. (Numbers correspond to thickness of the substrate in millimeter).

To eliminate far-field coupling, far-field radiation pattern of the antenna is used. The far-field radiation pattern of the antenna in Figure 4(a) is omnidirectional in the horizontal plane if the dielectric is replaced by air [18]. Since dielectric does not exist, there are no dielectric atoms to become polarized and hence affecting the radiation pattern.

This is shown in Figure 5. Replacing air by a dielectric constant of 2.2 affects the radiation in the horizontal direction. Therefore, antenna structure with a preferable low dielectric constant should be engineered in a way that there exists little radiation in the horizontal direction to side antenna element. Figure 5 shows the x - y plane radiation pattern of a two element array. The solid line is related to the pattern of the structure with air as the substrate. This shows an omnidirectional pattern. If air is replaced by a dielectric substrate, the dashed line in Figure 5 shows that the related radiation pattern has a peak towards the neighboring patch element. Through modifying the antenna structure, one can manipulate the radiation pattern in such a way that it would have null towards the neighboring patch element. Thus, the coupling between the two patches could be reduced.

Finally, near-field coupling is reduced by making antenna elements apart from each other more than a quarter of the longest operating wavelength of the antenna which guarantees no near-field coupling propagation.

In this paper, through bending the feed lines, placing a slot in the ground beneath the feed lines and adding a stub in between the patch elements, one can obtain improved isolation. These add-ons perfectly enhance isolation at the cost of a venial change of the radiation pattern. Through simulation one can justify the above. Figure 6 shows the S -parameters demonstrating the concept introduced.

To understand the antenna behavior, one can view the current distribution (see Figure 4). The current distribution results show that by introducing the proposed mechanism, once an element is fed, the neighboring element is hardly excited, confirming that mutual coupling is reduced between the elements. The related near-field distribution of the proposed antenna structure is shown in Figure 7. From Figure 7 it is crystal clear how near-field coupling changes by adding various parts to the proposed

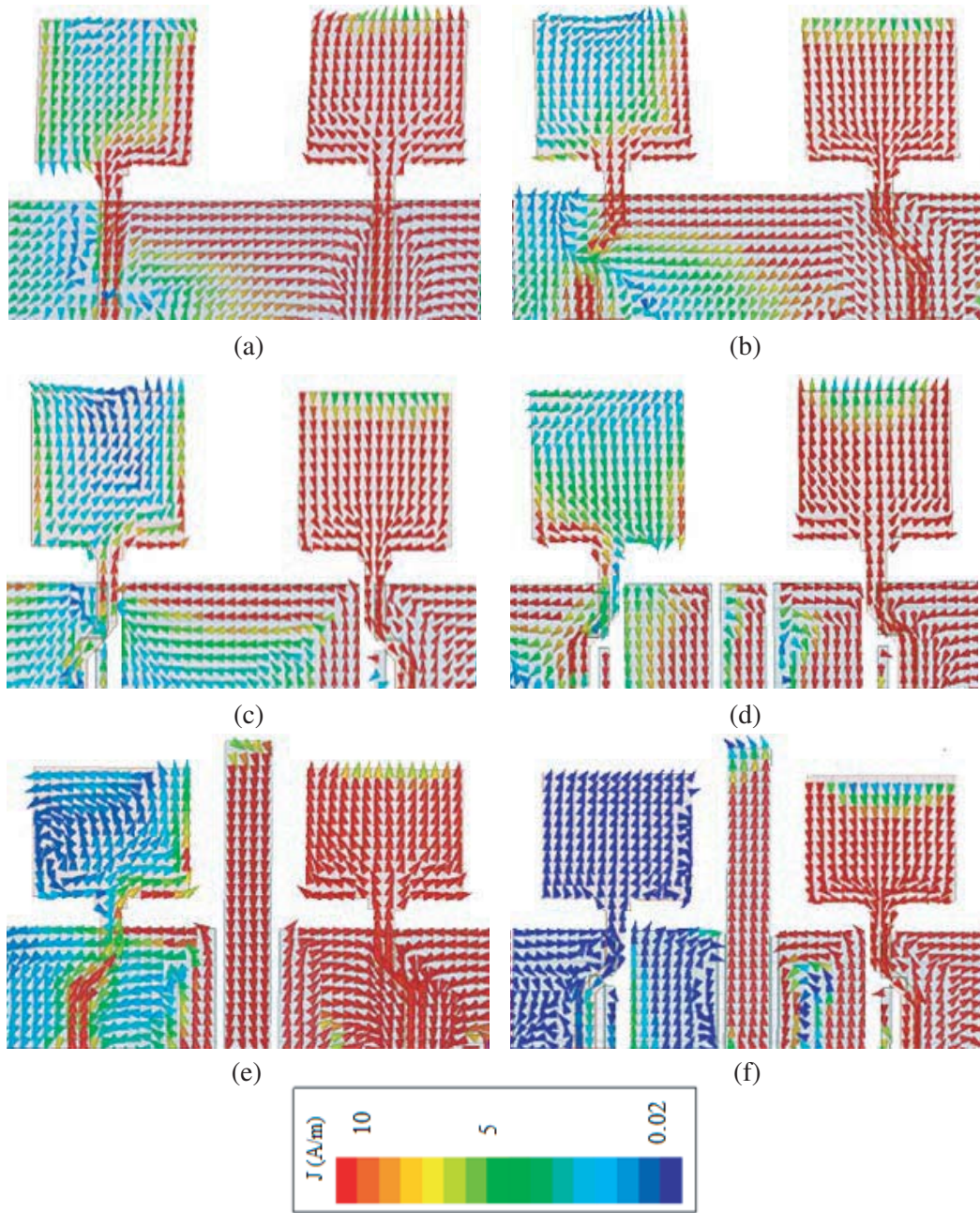


Figure 4. The current distribution of the proposed UWB MIMO antenna at 4.5 GHz. (a) The basic structure with no mutual coupling reduction technique. (b) Bending the feedline which results to reverse induced current. (c) H-shaped slots are applied to reduce near-field coupling. (d) The grounds are separated from each other. (e) A long strip is applied without H-shaped slots. (f) A long strip is applied with H-shaped slots.

UWB MIMO antenna. It is worth to mention that the modifications done to the array structure can have a slight effect on impedance matching of the antenna.

The S -parameters for different structures of the proposed UWB MIMO antenna is plotted in Figure 8. It is obvious from Figure 8 that using two H-shaped slots or a long ground stub between the two antenna elements independently can decrease S_{12} by 10 dB due to mutual coupling. This demonstrates the repeatability of the proposed method to apply to any structure.

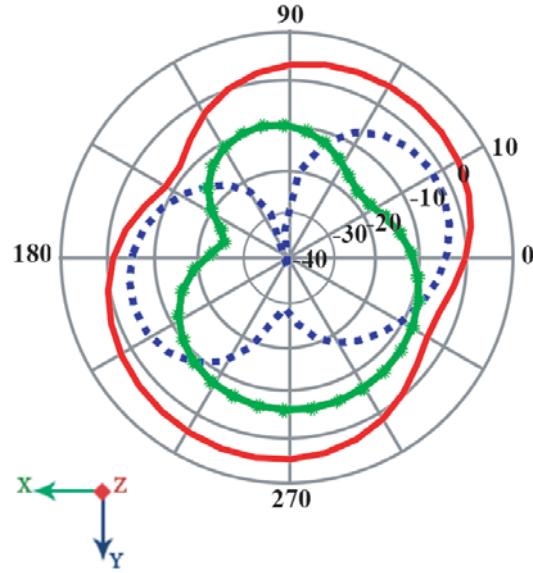


Figure 5. The horizontal radiation pattern of the patch antenna for red: configuration of Figure 4(a) and suspended in air; blue: configuration of Figure 4(a) with a substrate; green: configuration of Figure 4(f) with substrate. (Right port excited at 4.5 GHz, the other match).

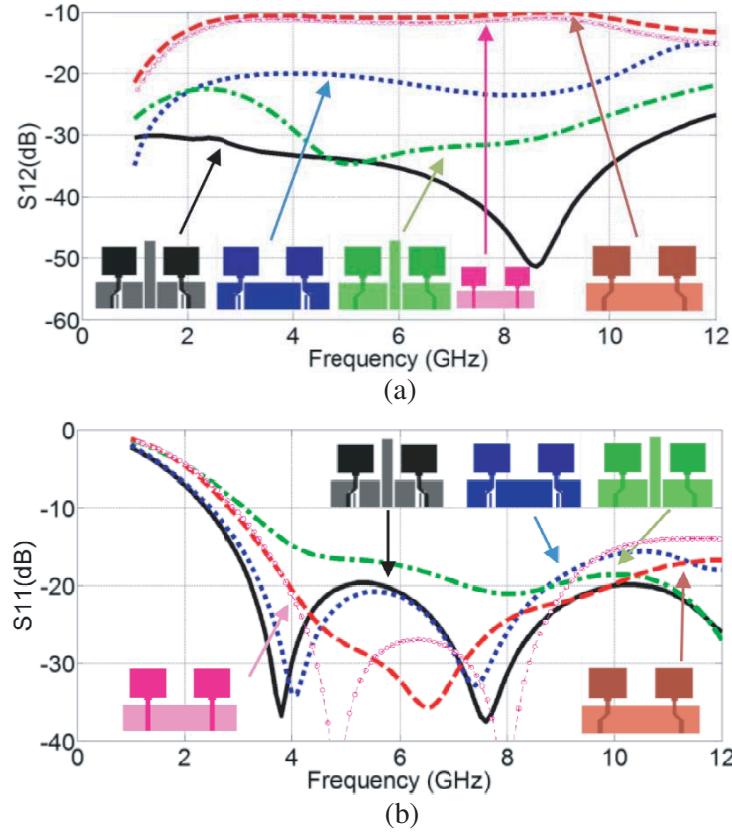


Figure 6. S -parameters of the different structures of the proposed UWB MIMO antenna. (a) S_{12} (dB). (b) S_{11} (dB).

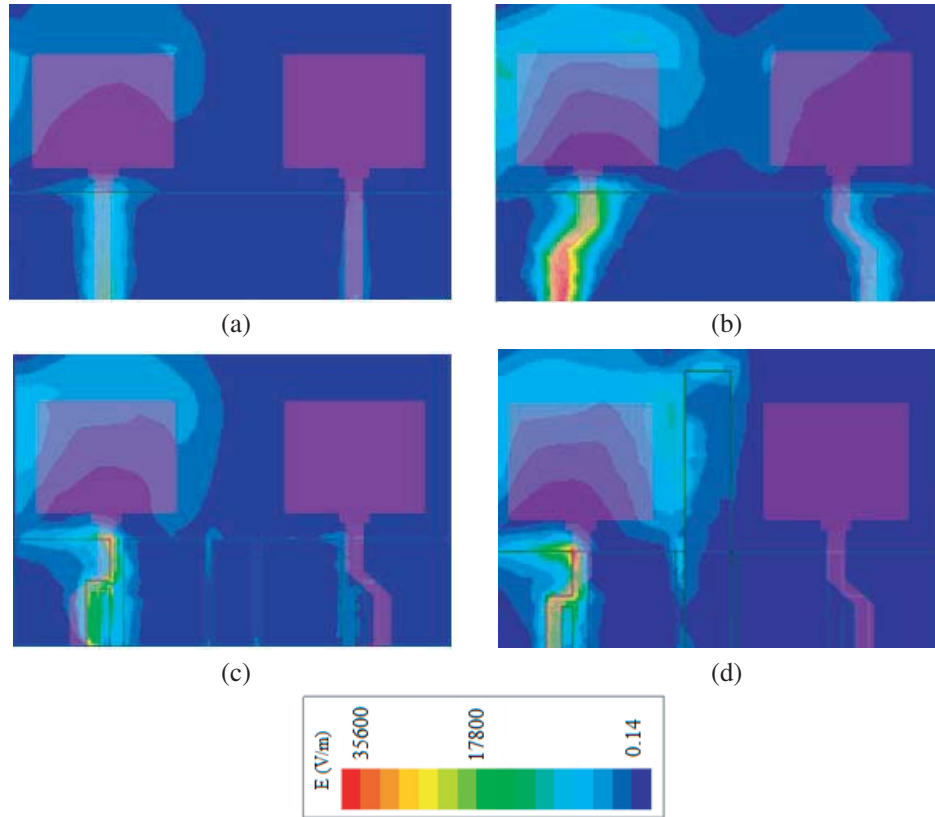


Figure 7. Near-field distribution of the proposed UWB MIMO antenna at 4.5 GHz. (a) The basic structure with no mutual coupling reduction technique. (b) Bending the feedline to separate antenna elements more efficiently. (c) H-shaped slots and ground separation are etched to improve isolation. (d) A long strip is applied to prevent near-field coupling to the side antenna element.

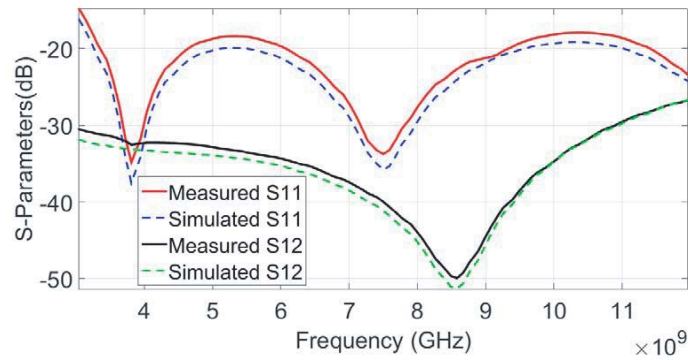


Figure 8. *S*-parameters of the proposed MIMO antenna.

4. RESULTS AND DISCUSSION

4.1. *S*-Parameters

The proposed MIMO antenna has been fabricated and tested. Computer simulation and measurement have been used to study the antenna performance. The simulated and measured *S*-parameters are in a good agreement as shown in Figure 8. The results in Figure 8 show an operation frequency from 3

to 12 GHz, and with the introduced technique, a mutual coupling of less than -25 dB is also achieved. A return loss better than 10 dB all over the bandwidth is mainly because electric field is quadratically related to current distribution near the edges, which is not considered in the HFSS simulation.

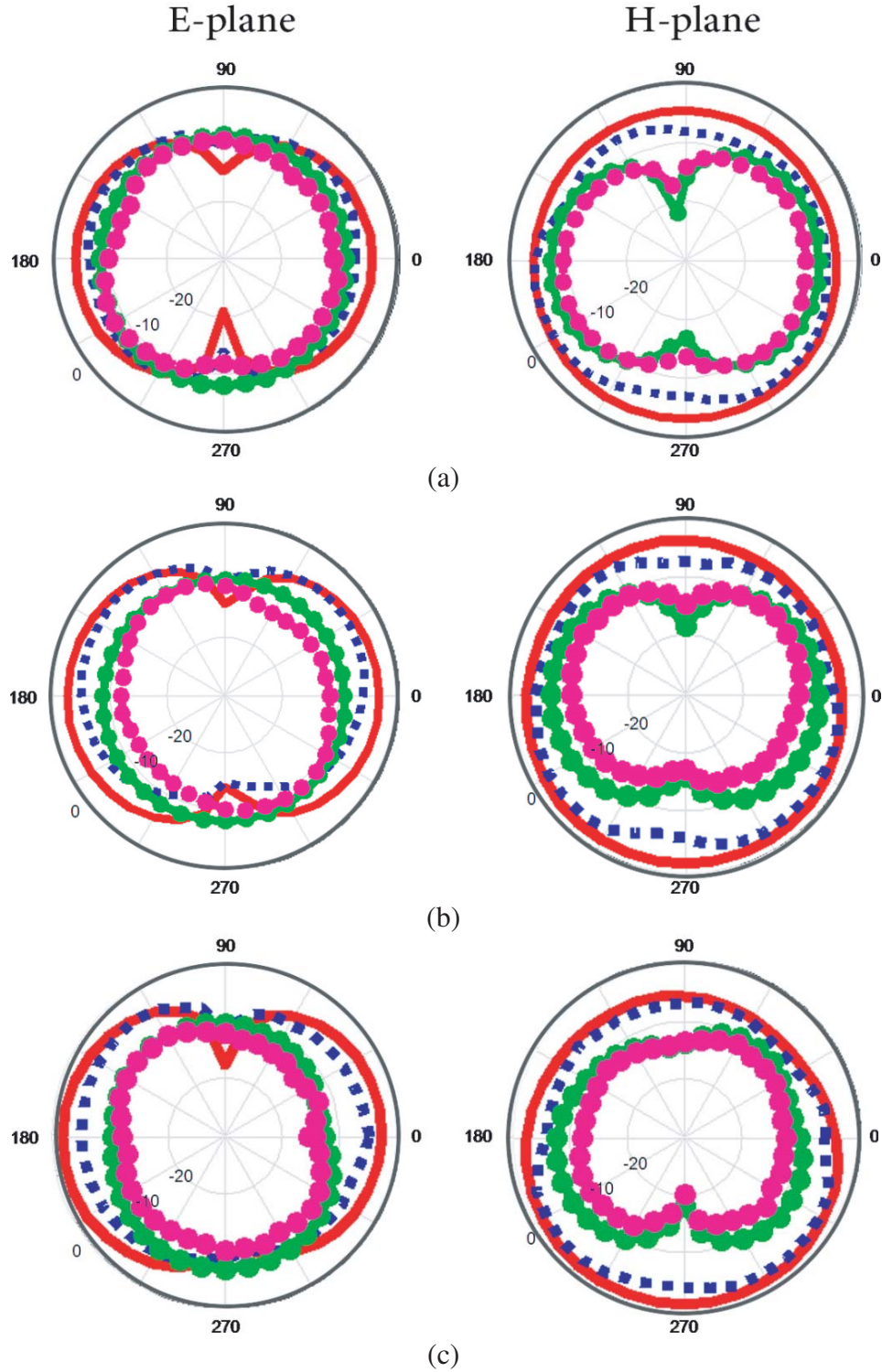


Figure 9. Measured E -plane and H -plane radiation patterns of the proposed two-element MIMO antenna at (a) 3.5, (b) 5 and (c) 8.5 GHz (red: co simulated; blue: co measured; green: cross simulated; pink: cross measured).

4.2. Radiation Pattern

The simulated and measured radiation patterns of the proposed MIMO antenna in the x - y (H -plane) and y - z (E -plane) planes at 3.5, 5 and 8.5 GHz are given in Figure 9. Patterns are obtained with one element fed and the other impedance matched.

At the frequency of 3.5 and 5 GHz, from Figures 9(a) and (b), it is observed that H -plane pattern is omnidirectional, and E -plane is also very stable with changes in frequency. At the high frequency of 8.5 GHz (Figure 9(c)), the H -plane pattern is sort of omnidirectional, but E -plane pattern is not very stable with changes in frequency.

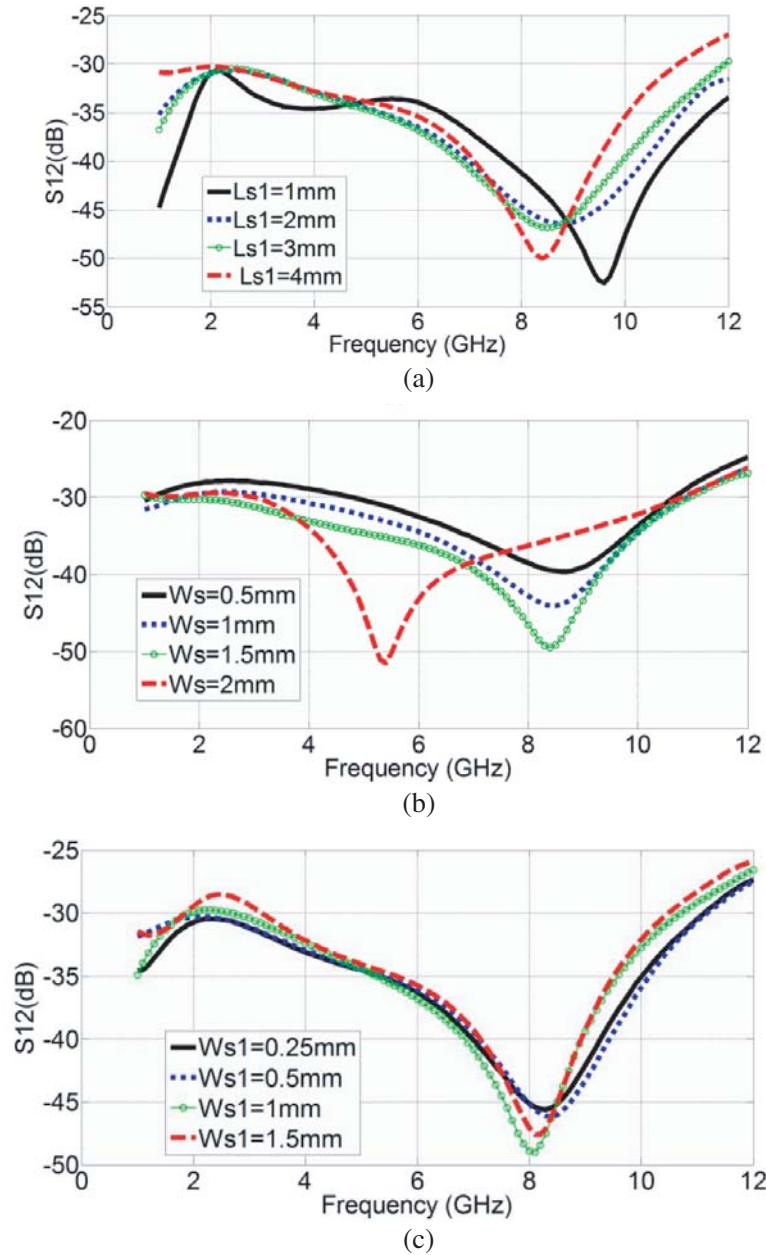


Figure 10. S_{12} parameter of the proposed UWB MIMO antenna for different parameters. (a) L_{S1} . (b) W_{S1} . (c) W_S .

4.2.1. Parametric Study

Different lengths and widths have also been studied in Figure 10. It is clear from Figure 10(a) that extending the width of L_{S1} shifts the corresponding resonance frequency toward longer wavelength which can be used to improve mutual coupling at low frequencies. Figure 10(b) indicates that varying W_{S1} has negligible effect on antenna performance. On the other hand, W_S parameter effectively shifts the resonance frequency of mutual coupling toward longer wavelength as W_S increases which is shown in Figure 10(c).

Separating the grounds also contributes to mutual coupling due to surface wave propagation at low frequencies. Figure 11 demonstrates that ground connection can significantly enhance isolation at low frequencies. Moreover, different separation sizes were also simulated and considered in which no significant contribution to the mutual coupling was observed. This reduction to mutual coupling due to ground connection in low frequency is based on the fact that at lower frequencies the wavelength is longer and therefore shifts the mutual coupling related S -parameter toward longer wavelength.

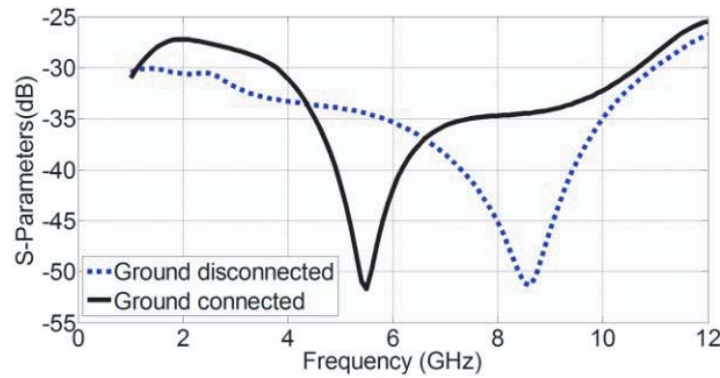


Figure 11. Simulated S_{12} for the connected and disconnected ground of the proposed UWB MIMO antenna.

4.3. Comparison of Reported Antenna Structures

The analysis of diversity performance has also been carried out on the proposed antenna which is shown in Figures 12 and 13. Envelope correlation of lower than 0.001 and capacity loss of fewer than 0.4 bps/Hz were achieved.

A comparison between the results reported in the available articles in the literature and the results obtained in the present work is given in Table 2. The proposed antenna of the present work has $S_{12} \leq -25$ dB throughout the bandwidth from 3.1 to 10.6 GHz with the parallel port position and

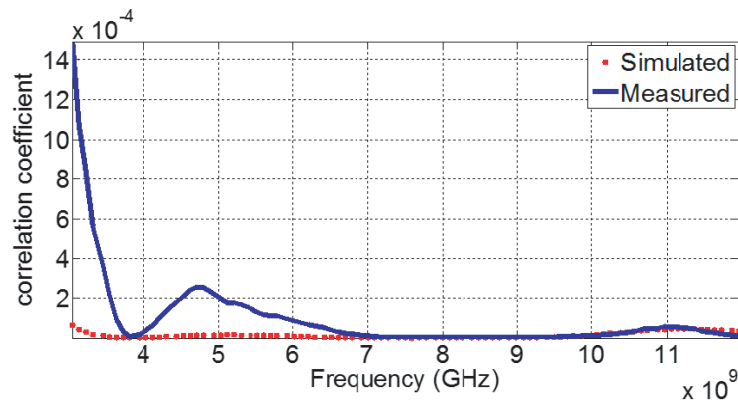


Figure 12. Envelope correlation of the MIMO using S -parameter [14]. (Diversity configuration of Figure 1).

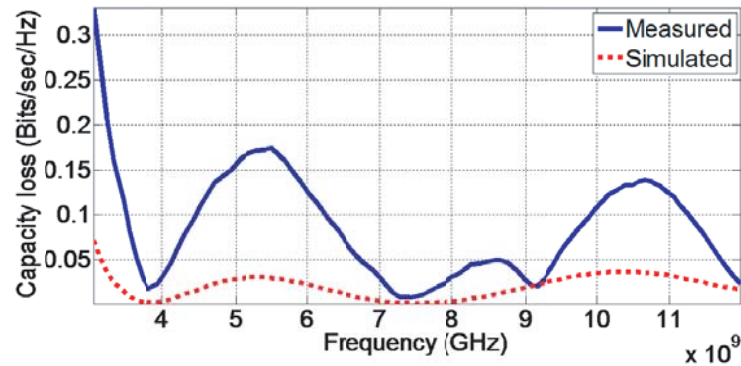


Figure 13. Measured and simulated capacity loss. (Configuration of Figure 1).

Table 2. Comparison of the present work and those of previously reported works.

Reference	Port position	Size comparison (Proposed/Reference)	Bandwidth ratio of Proposed/Reference $S_{12} < 20$ dB
[18]	vertical	42.44%	43%
[19]	parallel	69.90%	28%
[20]	parallel	44.94%	52%
[21]	parallel	37.5%	45%
[22]	parallel	66%	90%
[23]	parallel	57%	90%
[24]	parallel	55%	100%
[25]	parallel	120%	74%
[26]	parallel	90%	95%
[27]	parallel	50%	45%
Present work	parallel	100%	100%

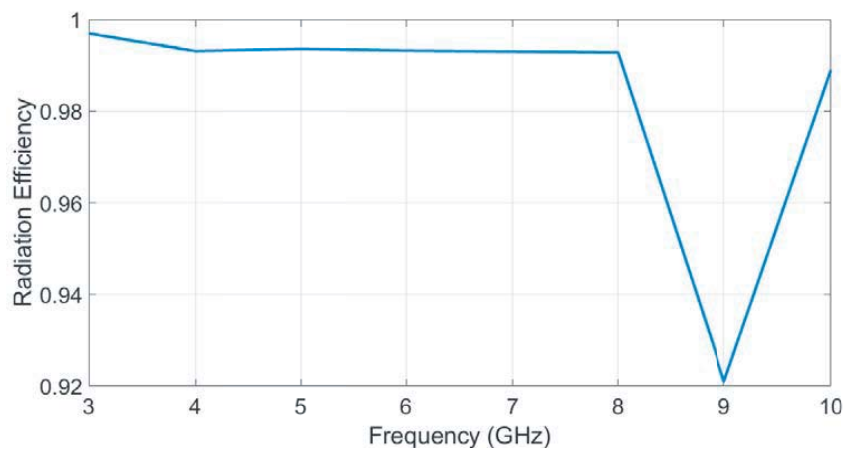


Figure 14. Simulated radiation efficiency of the proposed UWB MIMO antenna.

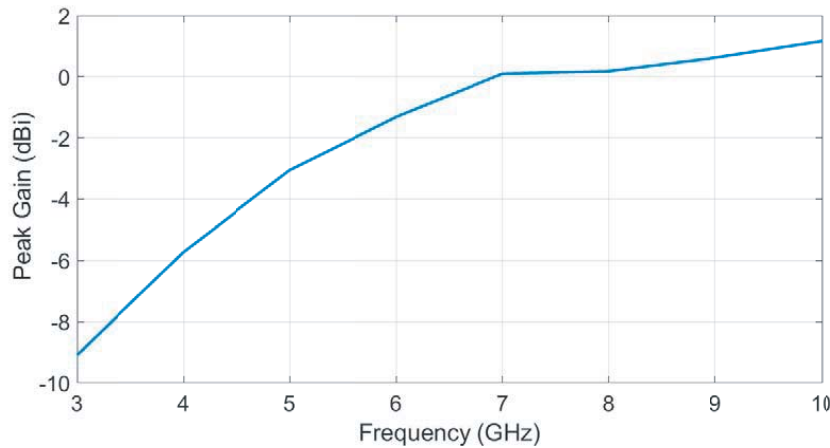


Figure 15. Simulated peak gain of the proposed UWB MIMO antenna.

simulated radiation efficiency of higher than 95%. These characteristics make the proposed antenna a good candidate for small size UWB applications. The radiation efficiency and peak gain of the proposed antenna are plotted in Figures 14 and 15, respectively.

5. CONCLUSION

A novel technique to improve isolation between two closely-spaced antenna elements was introduced. The proposed antenna with a small size of $30.1 \times 20.5 \text{ mm}^2$ and very high isolation with S_{12} less than -25 dB was presented. The technique improved isolation significantly, especially at low frequencies which is hard to achieve. This reduction was also demonstrated by using the simulation of current distribution. The proposed technique can be utilized easily in other multiple antenna structures. The simulated radiation efficiency of higher than 95% with a stable omnidirectional pattern at all three shown frequencies was also obtained. These results make the proposed antenna a good candidate for portable UWB application.

REFERENCES

1. FCC, First report and order, Federal Communications Commission, Washington, DC, 2002.
2. Hui, L., J. Xiong, Z. Ying, and S. L. He, "Compact and low profile co-located MIMO antenna structure with polarisation diversity and high port isolation," *Electronics Lett.*, Vol. 46, 108–110, 2010.
3. Liu, L., S. Cheung, and T. Yuk, "Compact MIMO antenna for portable devices in UWB applications," *IEEE Trans. Antennas Propag.*, Vol. 61, 4257–4264, 2013.
4. Nikolic, M. M., A. R. Djordjevic, and A. Nehorai, "Microstrip antennas with suppressed radiation in horizontal directions and reduced coupling," *IEEE Trans. Antennas Propag.*, Vol. 53, 3469–3476, 2005.
5. Ren, J., W. Hu, Y. Yin, and R. Fan, "Compact printed MIMO antenna for UWB applications," *IEEE Antennas Wireless Propag. Lett.*, Vol. 13, 1517–1520, 2014.
6. Tang, T. C. and K. H. Lin, "MIMO antenna design in thin-film integrated passive device," *IEEE Transactions Components Packaging and Manufacturing Technology*, Vol. 4, 648–655, 2014.
7. Arun, H., A. K. Sarma, M. Kanagasabai, S. Velan, C. Raviteja, and M. Alsath, "Deployment of modified serpentine structure for mutualcoupling reduction in MIMO antennas," *IEEE Antennas Wireless Propag. Lett.*, Vol. 13, 277–280, 2014.
8. Tang, T. C. and K. H. Lin, "An ultrawideband MIMO antenna with dualband-notched function," *IEEE Antennas Wireless Propag. Lett.*, Vol. 13, 1076–1079, 2014.

9. Gao, P., S. He, X. Wei, Z. Xu, N. Wang, and Y. Zheng, "Compact printed UWB diversity slot antenna with 5.5-GHz band-notched characteristics," *IEEE Antennas Wireless Propag. Lett.*, Vol. 13, 376–379, 2014.
10. Mohammad-Ali-Nezhad, S. and H. R. Hassani, "A novel tri-band E-shaped printed monopole antenna for MIMO application," *IEEE Antennas Wireless Propag. Lett.*, Vol. 9, 576–579, 2010.
11. Mohammad-Ali-Nezhad, S. and H. R. Hassani, "A penta-band printed monopole antenna for MIMO applications," *Progress In Electromagnetics Research C*, Vol. 84, 241–254, 2018.
12. Debnath, P., A. Karmakar, A. Saha, and S. Huda, "UWB MIMO slot antenna with Minkowski fractal shaped isolators for isolation enhancement," *Progress In Electromagnetics Research M*, Vol. 75, 69–78, 2018.
13. Jetty, C. R. and V. R. Nandanavanam, "Compact MIMO antenna with WLAN band-notch characteristics for portable UWB systems," *Progress In Electromagnetics Research C*, Vol. 88, 1–12, 2018.
14. Foudazi, A., A. R. Mallahzadeh, and S. Mohammad-Ali-Nezhad, "A triple-band WLAN/WiMAX printed monopole antenna for MIMO applications," *Microw. Opt. Technol. Lett.*, Vol. 54, 1321–1325, 2012.
15. Yang, X., Y. Liu, Y.-X. Xu and S. Gong, "Isolation enhancement in patch antenna array with fractal UC-EBG structure and cross slot," *IEEE Antennas Wireless Propag. Lett.*, Vol. 16, 2175–2178, 2017.
16. Rajo-Iglesias, E., O. Quevedo-Teruel, and L. Inclan-Sanchez, "Planar soft surfaces and their application to mutual coupling reduction," *IEEE Trans. Antennas Propag.*, Vol. 57, 3852–3859, 2009.
17. Wang, F., Z. Duan, S. Li, Z.-L. Wang, and Y.-B. Gong, "Compact UWB MIMO antenna with metamaterial-inspired isolator," *Progress In Electromagnetics Research C*, Vol. 84, 61–74, 2018.
18. Yook, J. G. and L. P. Katehi, "Micromachined microstrip patch antenna with controlled mutual coupling and surface waves," *IEEE Trans. Antennas Propag.*, Vol. 49, 1282–1289, 2001.
19. Kang, L., H. Li, X. Wang, and X. Shi, "Compact offset microstrip-fed MIMO antenna for band-notched UWB applications," *IEEE Antennas Wireless Propag. Lett.*, Vol. 14, 1754–1757, 2015.
20. Luo, C. M., J. S. Hong, and L. L. Zhong, "Isolation enhancement of a very compact UWB-MIMO slot antenna with two defected ground structures," *IEEE Antennas Wireless Propag. Lett.*, Vol. 14, 1766–1769, 2015.
21. Roshna, T., U. Deepak, V. Sajitha, K. Vasudevan, and P. Mohanan, "A compact UWB MIMO antenna with reflector to enhance isolation," *IEEE Trans. Antennas Propag.*, Vol. 63, 1873–1877, 2015.
22. Huang, H.-F. and S.-G. Xiao, "Compact UWB MIMO ground linearly tapered slot antenna decoupled by a stepped slot," *Progress In Electromagnetics Research C*, Vol. 71, 17–23, 2017.
23. Yadav, D., M. P. Abegaonkar, S. K. Koul, V. N. Tiwari, and D. Bhatnagar, "Two element band-notched UWB MIMO antenna with high and uniform isolation," *Progress In Electromagnetics Research M*, Vol. 63, 119–129, 2018.
24. Chandel, R., A. K. Gautam, and K. Rambabu, "Tapered fed compact UWB MIMO-diversity antenna with dual band-notched characteristics," *IEEE Trans. Antennas Propag.*, Vol. 66, 1677–1684, 2018.
25. Tao, J. and Q. Feng, "Compact ultrawideband MIMO antenna with half-slot structure," *IEEE Antennas Wireless Propag. Lett.*, Vol. 16, 792–795, 2017.
26. Gautam, A. K., S. Yadav, and K. Rambabu, "Design of ultra-compact UWB antenna with band-notched characteristics for MIMO applications," *IET Microwaves, Antennas & Propagation*, Vol. 12, 1895–1900, 2018.
27. Khan, M. S., A. Capobianco, S. M. Asif, D. E. Anagnostou, R. M. Shubair, and B. D. Braaten, "A compact CSRR-enabled UWB diversity antenna," *IEEE Antennas Wireless Propag. Lett.*, Vol. 16, 808–812, 2017.